Tunnelling for a Better Life – Yan, Celestino, Thewes & Eberhardt (Eds)

Planning and support estimation of underground powerhouse in the Himalayas

Sailesh Adhikari*
Norwegian University of Science and Technology, Trondheim, Norway
Tribhuvan University, IOE, Pashchimanchal Campus, Pokhara, Nepal

Chhatra Bahadur Basnet
Tribhuvan University, IOE, Pashchimanchal Campus, Pokhara, Nepal

Krishna Kanta Panthi
Norwegian University of Science and Technology, Trondheim, Norway

Tek Bahadur Katuwal
Norwegian University of Science and Technology, Trondheim, Norway
Tribhuvan University, IOE, Pashchimanchal Campus, Pokhara, Nepal

ABSTRACT: Underground structures like tunnels and caverns have major advantages in hydropower projects. Tunnels are used for transporting the water from the intake to the tailrace outlet through the turbines whereas caverns primarily serve the purpose of powerhouse, transformer caverns, and settling basins. The site selection of the underground cavern is an important task to be considered to optimize the rock support and cost. Design aspects regarding stability and functionality are governed by the location, orientation, shape, and size of the caverns. Similarly, the choice of support for a particular geological condition and type and quality of rock mass needs to be carefully assessed during planning and implemented during the construction. This article discusses the location design and rock support requirement of the underground powerhouse cavern of the Super Dordi Hydropower Project in Nepal. The project lies in the lower boundary of the Higher Himalayan rock formation. The powerhouse cavern has a length of 39 m and has width (span) and height of 14.5 m × 28 m, respectively. The rock support measures predicted during planning are modelled using 2D numerical modelling tools. The study on monitored data and numerically modelled data are compared and discussed.

Keywords: Underground Space, Support Characteristics, Deformation, Powerhouse Cavern, Himalayan Rock Mass

1 INTRODUCTION

The use of underground spaces has significantly increased in various engineering projects. The development of underground spaces has advantages like no impact on the landscape, very little or almost no disturbance to the surface human activities and resources, higher safety level, etc. It is particularly important in places where natural hazards like landslides and earthquakes are bound to occur. Nepal, a mountainous country, suffers various hazards posing a challenge to develop various infrastructure projects. Having a high potential for hydropower development, the sustainable development of the various structures for hydropower plants is the major issue to be addressed by the engineers in Nepal. The best alternative to protect structures from natural calamities like landslides and earthquakes is to make the components underground. The varied geological conditions and challenging terrains demand special attention to the construction of underground structures in Nepal. The tectonically active rock mass in the Himalayan region has the presence of weak, highly deformable, and anisotropic rock mass with a high degree of weathering and fracturing (Panthi and Nilsen, 2007), posing challenges for the construction of tunnels and caverns. Location, orientation, geometry, complexity of access tunnels, and geological conditions are major factors to be considered

*Corresponding author: sailesh.adhikari@ntnu.no

DOI: 10.1201/9781003495505-417

during the evaluation of stability and planning of underground structures (Rathore and Panthi, 2017). Project-specific characteristics like size, shape, location, and orientation influences the design of caverns and tunnels. (Panthi, 2006). Further, the stability is dependent on the rock mass quality, in-situ stress, and groundwater conditions.

The Himalayan Mountain series was formed due to the subduction of the Indian plate to the Tibetan plate. There are five major subdivisions of the tectonic boundaries in the Himalayan region. The major subdivisions from the southern belt towards the northern belts are the Gangetic plane (Terai), Siwaliks zone, Lesser Himalayan zone, Higher Himalayan zone, and Tibetan-Tethys zone. These divisions span approximately in the NW-SE directions. The subdivisions are separated by the boundaries of the main frontal thrust (MFT), main boundary thrust (MBT), and main central thrust (MCT). These tectonic zones are all characterized by special lithology, tectonics, geological structures, and geological history and are made up of different rock types (Panthi, 2006). Figure 1 shows the simplified geological map of Nepal with the geological and tectonic boundaries.

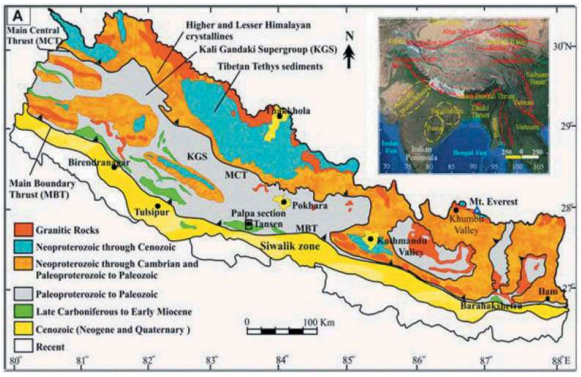

Figure 1. Geologic subdivisions of Himalayas (ref. Khatri et al., 2021).

In the lower boundary of higher Himalayas, i.e. near MCT (project site location of the present case study) the rocks of highly sheared, intensely deformed, and mylonitized green-schist and schistose mica gneiss are present (Robyr et al, 2002). Rock masses in the Himalayan region are influenced by faulting, folding, schistosity, and jointing to varying degrees representing geological complexity (Basnet and Panthi, 2020). In underground openings, the excavation-induced response of the rock mass may arise instability conditions. This paper discusses the design and support estimation of the powerhouse cavern of Super Dordi Hydropower Project (SDHP) located in Lamjung district of Nepal. The project lies in the higher Himalayas zone about 10 km north of MCT. The dimension of the powerhouse cavern is about 39 m × 14.5m × 28m. The powerhouse cavern has an arched roof and vertical walls. The dimensions of the powerhouse were optimized to accommodate the turbine, distribution pipes, and other construction areas based on the dimensions of the various machinery components.

2 BRIEF DESCRIPTION OF THE PROJECT

SDHP is a run-of-river type hydropower project with an installed capacity of 54 MW. The project has a gross head of 638 m. The project lies in the lower boundary of the higher Himalayan rock formation and facilitates a diversion weir (18.5 m long) and intake, double-chambered underground settling basin caverns (each having approximate cross-section area 113 sq. m), gravel trap (33.5 m long), headrace tunnel (4.7 km long), access tunnels, surge shaft (49 m high and 6 m diameter), penstock shafts (1052 m long), powerhouse cavern, and tailrace tunnel. Most of the civil structures of the project are underground except the diversion weir and switchyard. The project area consists of medium to high-grade metamorphic rocks like schist and gneiss and the feasibility study showed that there was no severe geological risk associated with the project (PHCPL, 2012). Figure 2 shows the project layout plan of SDHP with the location of different components of the hydropower project.

Initially, the powerhouse was proposed to be at the surface instead of underground. However, during the earthquake in April 2015, there was a small landslide near the uphill area of the old powerhouse site. The powerhouse will store heavy machinery and expensive equipment; thus, it was too risky to build the powerhouse on the surface. Eventually, it was decided to build the underground powerhouse instead of the surface powerhouse (Panthi, 2018). During construction, a shear band of about 10 to 20 cm was encountered near the powerhouse cavern location. The cavern location was further pushed by about 40m inside the mountain to minimize the impact. The alignment of underground structures is an important parameter to be addressed during the construction of tunnels and caverns. Poor alignment will lead to unusual overbreak, water ingress, and increased risk to health and safety (Katuwal et al., 2023). The rock mass encountered in the powerhouse cavern was of good quality. Two main joint sets with occasional random joints were mapped. These joints have medium persistence, spacing varying between 2.5 to 3m, and tight fillings with clay and silt. The orientation of the powerhouse cavern is N45E and is favourable in terms of major joint sets. Figure 3 shows the joint rosette with a cavern length axis (Panthi, 2018). The rock mass was relatively dry in the powerhouse area with exceptions in the locations from chainage +025 to +030m where minor dripping of water was seen causing dry to damp conditions. The site selection of the powerhouse cavern is suitable in terms of major critical factors influencing the stability and support systems applied in the cavern.

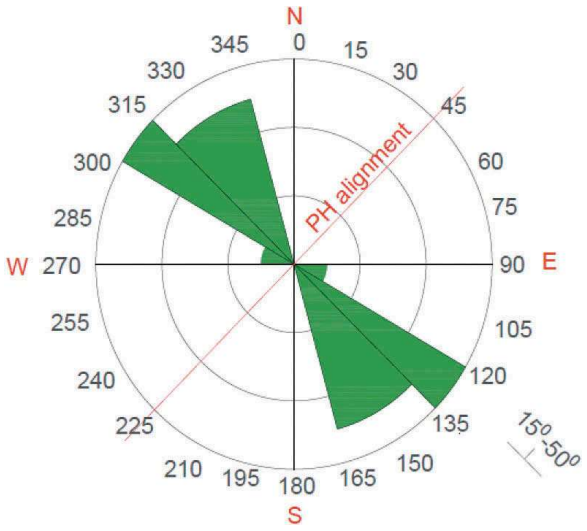

Figure 2. Project layout of SDHP.

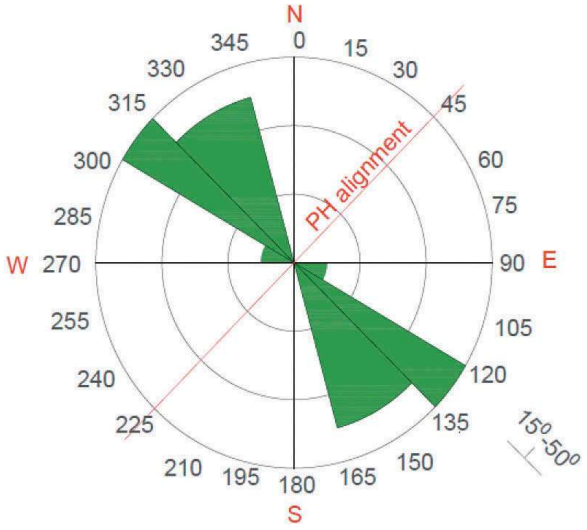

Figure 3. Joint rosette of the powerhouse cavern.

3 ROCK MASS QUALITY PARAMETERS

The rock parameters are established based on the geological mapping, laboratory test results of the intact rock, and some empirical relationships. Rock mass strength and deformation modulus, and choice of failure criteria govern the design of underground caverns. The geometry and rock support provided for the powerhouse cavern are shown in Figure 4. The three-layer fiber-reinforced shotcrete, with a final thickness of 15 to 20 cm depending upon rock condition and systematic bolting was provided as rock support. The rock bolts were installed in two stages. The first stage consisted of 5 m long cement grouted rock bolts of 25 mm diameter placed at the staggered arrangements at the spacing of 3m. In the second stage, 8 m long cement grouted rock bolts with 25 mm diameter were provided at a spacing of 3 m in a staggered pattern.

3.1 *Intact rock properties*

The laboratory results of the rock core samples from the project area show the mean uniaxial compressive strength of the samples was 112.6 MPa with a standard deviation of 8.65 MPa. Similarly, Young's modulus was 48.53 GPa with a standard deviation of 5.05 GPa. The average Poisson's ratio of the intact rock was 0.33 and the unit weight of the rock was found to be 2.7 t/m^3.

3.2 *Rock mass properties*

The strength and deformability properties of the rock mass are important parameters for modelling the tunnels and caverns. Additionally, the presence of weakness zone, shear zone, and 3D topography are influencing parameters to model the caverns (Adhikari et al. 2022).

3.2.1 *Rock mass quality*

The rock mass quality was assessed using Q-system of rock mass classification (Barton et. al., 1974). Table 1 shows the range of values and typical mean for the different parameters mapped at the cavern for the determining overall rock mass quality class.

The Q value of the rock mass ranges from 10 to 12 with the typical mean value of 10.5. This indicates the rock mass at the powerhouse cavern is of good quality.

3.2.2 *Compressive strength of rock mass*

Various researchers have provided different relationship between intact rock strength and rock mass strength. The most common ones are Bieniawaski (1993), Hoek et al. (2002), Barton (2002) and Panthi (2017), listed in Equations 1 to 4, respectively.

$$\sigma_{cm} = \sigma_{ci} \times \exp\left(\frac{\mathrm{RMR} - 100}{18.5}\right) \text{ and } \mathrm{RMR} = 9 \times \ln \mathrm{Q} + 44 \quad (1)$$

$$\sigma_{cm} = \sigma_{ci} \times \left[\exp\left(\frac{\mathrm{GSI} - 100}{9}\right)\right]^{a} \quad (2)$$

$$\sigma_{cm} = 5\gamma\left[\frac{\sigma_{ci}}{100} \times Q\right]^{1/3} \quad (3)$$

$$\sigma_{cm} = \frac{\sigma_{ci}^{1.6}}{60} \quad (4)$$

The results of the rock mass strength achieved by the above relationships is illustrated in Figure 5. Based upon the field mapping results and site conditions the value of GSI was considered 60.

It can be seen from Figure 5 that the empirical relationships from Bieniawaski (1993) and Hoek et al. (2002) give a lower value for the rock mass strength whereas the empirical relationships by Barton (2002) and Panthi (2017) give a higher values. For the

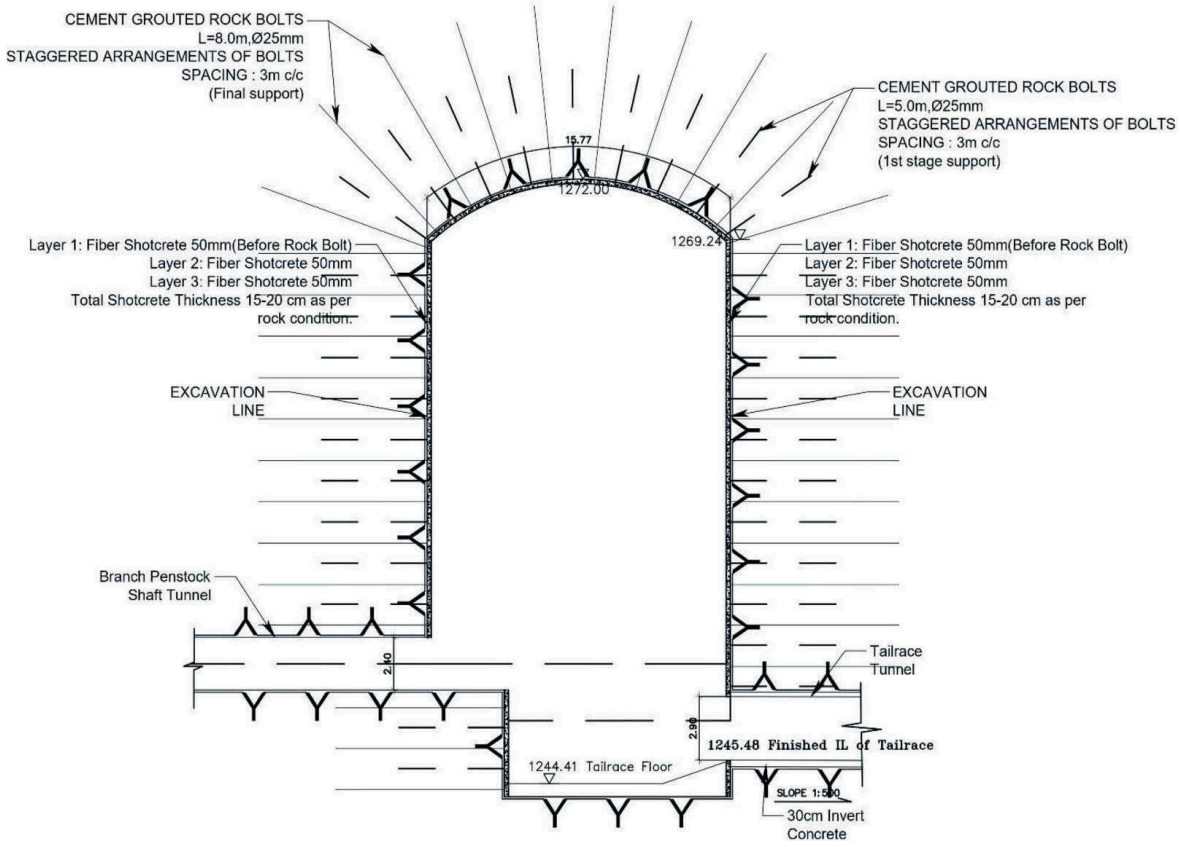

Figure 4. Support system provided in powerhouse cavern.

Table 1. Q-system of rock mass classification.

Parameters	Symbol	Value	
		Range	Typical Mean
Rock Quality Designation	RQD	60 – 80	70
Joint Set Number	J_n	3 – 6	4
Joint Roughness	J_r	1.5 – 3	2
Joint Alteration	J_a	2 – 4	3
Joint Water Reduction	J_w	0.8 – 1	0.9
Stress Reduction Factor	SRF	1	1
$Q = \frac{RQD}{J_n} \times \frac{J_r}{J_a} \times \frac{J_w}{SRF}$		10 – 12	10.5

homogeneous and relatively strong rock mass like at SDHP, the relationship between the intact rock strength and the strength of rock mass provided by Panthi (2017) is considered to be relevant and applicable. Unlike other relationships to compute the rock mass strength, the relationship is mainly based on lab-tested data and has no dependency on the rock mass classification system. Hence, the method eliminates the dependency on several other subjective parameters that depend upon the judgment of the engineer. Thus, an average rock mass strength is taken as 31.94 MPa for further analysis.

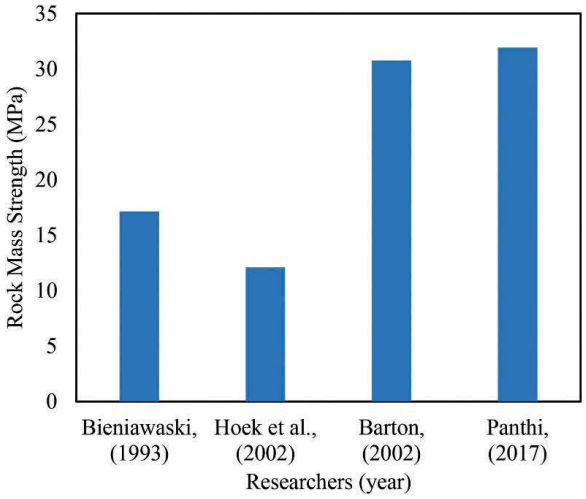

Figure 5. Rock mass strength by empirical relationship.

3.2.3 *Deformation modulus of rock mass*

The deformation modulus of the rock mass is also computed by the empirical relationship owing to the higher cost and measurement difficulties in the in-situ conditions. Like the compressive strength of rock mass, various researchers have provided the empirical formula to calculate the deformation modulus of rock mass. The relationship established by Bieniawaski (1978), Hoek et al. (2002), Barton

(2002), and Panthi (2006) is given from Equations 5 to 8 respectively.

$$E_m = 2RMR - 100 \tag{5}$$

$$E_m = \left(1 - \frac{D}{2}\right)\sqrt{\frac{\sigma_{ci}}{100}}\, 10^{\left(\frac{GSI-10}{40}\right)} \tag{6}$$

$$E_m = 10 \times \left(\frac{Q \times \sigma_{ci}}{100}\right)^{1/3} \tag{7}$$

$$E_m = E_{ci} \times \left(\frac{\sigma_{cm}}{\sigma_{ci}}\right) \tag{8}$$

In the above equation, E_m is the deformation modulus of rock mass, E_{ci} is the Youngs' modulus of the intact rock and σ_{ci} is the strength of the intact rock. The value of the deformation modulus obtained from the empirical relationship is illustrated in Figure 6. It is observed that the relationship provided by Bieniawaski (1978) provides the highest value of the deformation modulus and the relationship by Hoek et al (2002) and Panthi (2006) provides almost similar values. In this article, the deformation modulus obtained from Equation 8 proposed by Panthi (2006) is considered. The relationship is more suitable for the isotropic, homogeneous, and massive rock mass from the Himalayas. The deformation modulus of the rock mass computed is 13.76 GPa and is used as an input parameter for the numerical modelling of the cavern.

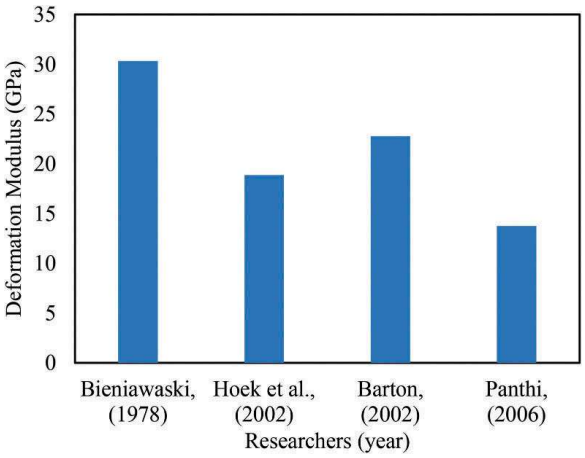

Figure 6. Deformation modulus by empirical relationship.

3.3 *Hoek Brown parameters*

GSI values are calculated by using the Q-systems' parameters using the following relationship (Hoek et al., 2013).

$$GSI = \frac{52(J_r/J_a)}{1 + (J_r/J_a)} + \frac{RQD}{2} \tag{9}$$

GSI was computed in the range of 53 to 63, which also matched the field mapping results to compute GSI. Hoek-Brown constant m_b, s and a are dependent upon the rock mass characteristics. These parameters are computed using the relationship from Equation 10 – 12.

$$m_b = m_i \times e^{\left(\frac{GSI-100}{28-14D}\right)} \tag{10}$$

$$s = e^{\left(\frac{GSI-100}{9-3D}\right)} \tag{11}$$

$$a = \frac{1}{2} + \frac{1}{6}\left(e^{-\frac{GSI}{15}} - e^{-\frac{20}{3}}\right) \tag{12}$$

Based on the site conditions during excavation and the chart provided by Hoek (2007), the value of the disturbance factor (D), which is dependent upon the blast damage to the contour is considered 0.6. Similarly, a GSI value of 60 and m_i value of 23 are considered to obtain the m_b, s, and a parameter. The residual GSI is assumed to be 20.

The values obtained for the disturbed and undisturbed zone are (m_b = 5.512, s = 11.7×10^{-3} and a = 0.503) and (m_b = 2.998, s = 3.86×10^{-3} and a = 0.503), respectively.

4 EVALUATION OF ROCK STRESSES

The in-situ rock stresses are generated due to the combination of gravitational load with tectonic stresses, topographic stresses, and residual stresses. According to Panthi (2012), the vertical and horizontal stresses on the rock mass can be computed as:

$$\sigma_v = \gamma H \tag{13}$$

$$\sigma_h = \frac{\nu}{1-\nu} \times \sigma_v + \sigma_{tec} \tag{14}$$

In the above equations, γ is the density of the rock, H is the overburden height, ν is the Poisson's ratio, and σ_{tec} is horizontal the tectonic stress in the rock mass.

In-situ stresses are measured by different methods like hydraulic fracturing, flat jack test, 3D overcoring test, etc. For the horizontal tectonic stress, no direct test was performed in the field. Instead, the horizontal tectonic stress of 4.5 MPa was assumed based on the tectonic stress of the headrace tunnel of the Upper Tamakoshi Hydropower Project (UTHP) (Panthi and Basnet, 2018) and Parbati-II Hydropower Project (Panthi, 2012) located in a similar tectonic regime and geological formation of the Higher Himalaya (Adhikari et al., 2023). From the World stress map the orientation of the tectonic stress is approximately N10E at the project location site. The

total horizontal stress is computed by resolving the tectonic stress and the horizontal stress due to gravity. Figure 7 shows a simple illustration of the computation for in-plane and out-of-plane horizontal stresses acting on the cavern. The angle between the horizontal tectonic stress regime and the cavern is 35°. The in-plane horizontal stress and out-of-plane horizontal stress are given by Equation 15 and Equation 16 respectively (Basnet and Panthi, 2020).

$$S_{yy} = S_{Hmax}\cos^2\theta + S_{Hmin}\sin^2\theta \quad (15)$$

$$S_{xx} = S_{Hmax}\sin^2\theta + S_{Hmin}\cos^2\theta \quad (16)$$

Based on the above data and the relationship provided in Equation 13 – 16, the in-situ stress parameters for the rock mass of the powerhouse cavern are summarized in Table 2.

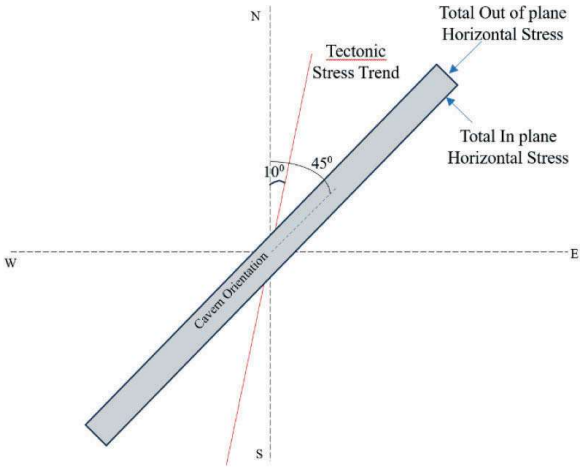

Figure 7. Illustration of the total horizontal stress for the cavern.

Table 2. In-situ stress parameters for rock mass of cavern.

Parameters	Value	Unit
Overburden Depth (H)	335	meters
Poisson's Ratio (ν)	0.31	-
Tectonic Stresses (σ_{tec})	7.5	MPa
Tectonic Stress Trend	N10°E	-
Cavern Alignment	N45°E	-
Unit Weight of Rock	2.7	t/m^3
Total Vertical Stress	9.05	MPa
Total Horizontal Stress	11.56	MPa

5 NUMERICAL MODELLING OF THE CAVERN

Numerical modelling of the powerhouse cavern is done by using the finite element method using RS2. The cavern is simulated as a continuum model where the whole rock mass is considered as a single homogeneous mass. The principal stresses and their orientations are computed by creating the valley model. Further, these stresses are then used as input parameters in the box model to compute the deformation and the support details of the cavern.

5.1 *Valley model to determine stresses in the rock mass*

The valley model as per the site condition is shown in Figure 8. This 2D model considers the topographic effects and the horizontal tectonic stress effects. The resolved stress in-plane and out-of-plane are given as input to compute the principal stresses. The results show that the value of major principal stress (σ_1) is 10.80 MPa, and minor principal stress (σ_3) is 6.27 MPa. The direction of the major principal stress to the horizontal axis is 55°. These values are adopted to compute the deformation in the powerhouse cavern by creating the box model of the cavern.

5.2 *Rock support details of the powerhouse cavern*

The support details as shown in Figure 4 are provided to the model of the powerhouse cavern. The supports provided are fiber-reinforced shotcrete, concrete, and systematic rock bolts, the details of which are summarized in Table 3.

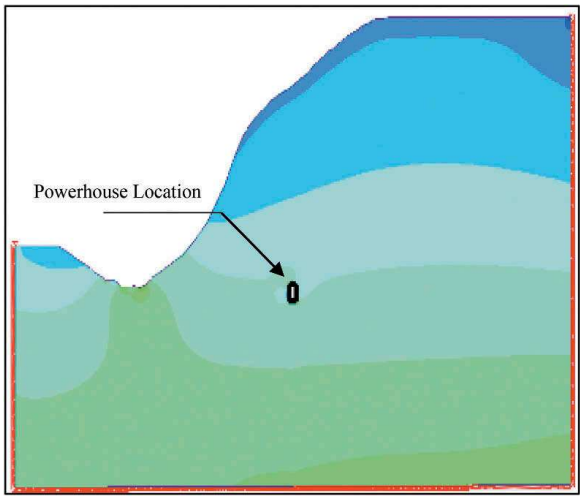

Figure 8. Valley model to compute principal stress for the cavern.

5.3 *Powerhouse cavern model*

The cavern model for powerhouse is made by taking the external boundary of the rock mass as 5 times the size of the cavern excavated. The disturbed zone of 2 meters from the excavation face is considered. The box model of the powerhouse cavern is shown in Figure 9. The support parameters and the stress parameters discussed previously are given as input to the model.

Table 3. Support parameters for cavern.

Shotcrete and Concrete Details:		
Support	Shotcrete	Concrete
Type	Standard Beam	Standard Beam
Compressive Strength	30 MPa	30 MPa
Tensile Strength	5 MPa	5 MPa
Poisson's Ratio	0.3	0.3
Rock Bolt Details:		
Support		Bolt
Type		Fully Bonded
Diameter		25 mm
Length		5m and 8m
Tensile capacity		0.1 MN

The crown of the powerhouse is at 1272 m from the mean sea level. The deformation was obtained numerically in the elevation 1267.6 m of the powerhouse cavern. The reading was computed in this location because the deformation in the powerhouse cavern was recorded using borehole extensometers at these locations. The deformation contour of the cavern is shown in Figure 10. The deformation obtained from numerical modelling and the borehole extensometer are shown in Table 4. The deformation values obtained from numerical modelling vary with the site-measured data but lie within an acceptable limit. The values are obtained for the chainage 15m from the instrument location.

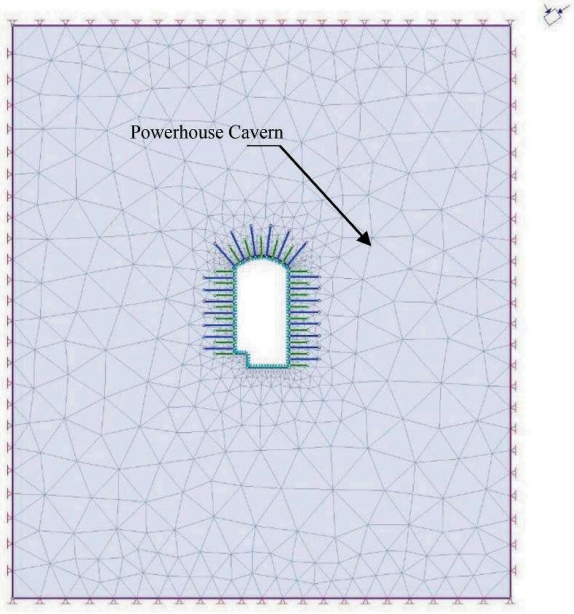

Figure 9. Box model of the cavern.

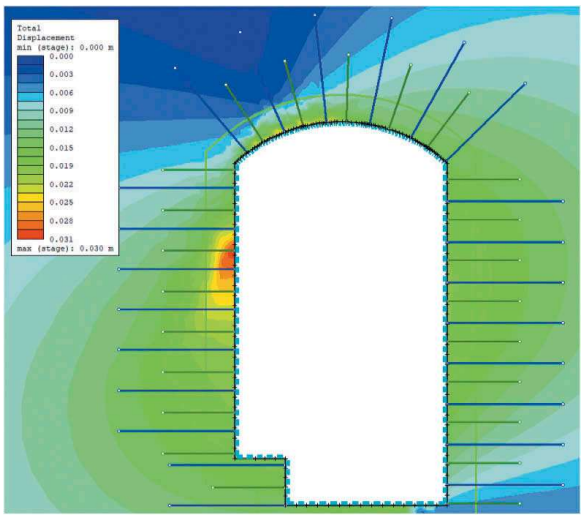

Figure 10. Deformation contour on the cavern.

Table 4. Deformation on the cavern.

Elevation	Wall	Numerical model value	Field Reading
1267.60 m	Left	6 mm	5.7 mm
	Right	5 mm	1.12 mm

6 DISCUSSIONS

The planning of a powerhouse cavern is dependent upon various factors like geometry (shape and size), topography, in-situ stress conditions, rock mass strength, rock mass quality, etc. These parameters must be properly assessed before excavating underground structures like tunnels and caverns. Field mapping and numerical modelling are the key steps to plan the initial support system and determine the magnitude and orientation of principal stresses. The deformation values obtained from the numerical model and the site measurement show the variation in the reading. It is mainly because deformation is affected by parameters prevailing in 3D conditions (geometry, topography, in-situ stresses, etc.). However, in the numerical modelling, only 2D finite element model is considered which lacks the exact situations of the ground conditions based on 3D parameters. Nevertheless, the magnitude from numerical modelling and site does not differ significantly to cause stress-induced instability in the caverns. Thus, 2D numerical model can be used as a tool to predict the deformation behaviour of the underground openings.

7 CONCLUSIONS

This paper discussed the geological conditions, layout, and location of the powerhouse cavern, used rock support, and the deformation characteristics of

the rock mass surrounding the powerhouse cavern of Super Dordi Hydropower Project located in the lower boundary of the higher Himalayan rock formation at Lamjung district of Nepal. The planning and design carried out for this cavern were very suitable in terms of shape, size, and potential weakness zone. The cavern is now in use and no significant deformations and other challenges in the applied rock support are seen at the site. The support provided is sufficient to make the cavern long-term stable and will serve its functional purpose for many decades to come.

ACKNOWLEDGMENTS

This research was supported by NORHED II Project 70141 6; Capacity Enhancement in Rock and Tunnel Engineering at the Pashchimanchal Campus (WRC), Institute of Engineering (IoE), Tribhuvan University (TU), Nepal. The authors acknowledge NORAD, Norway for funding the project and providing financial help for site visits and conducting this research. The authors are also thankful to People's Hydropower Company (P) Ltd. for providing necessary data to publish this work.

REFERENCES

Adhikari, S., Panthi, K.K. & Basnet, C.B., 2023. Stability issues associated with the construction of underground caverns of Super Dordi Hydropower Project, Nepal. ISRM 15th International Congress on Rock Mechanics and Rock Engineering – Challenges in Rock Mechanics and Rock Engineering, Salzburg, Austria, ISBN 978-3-9503898-3-8

Adhikari, S., Basnet, C.B., and Shrestha, G.B., 2022. Rock Excavation and Support for an Underground Powerhouse Cavern at Super Dordi Kha Hydropower Project, Nepal. Proceedings of 12th IOE Graduate Conference, Vol. 12, pp. 291–298 ISSN: 2350-8914

Barton, N., Line, R. & Lunde J., 1974. Engineering classification of rock masses for the design of tunnel support. Rock Mechanics, Vol. 6, pp 189–236, https://doi.org/10.1007/BF01239496

Barton, N., 2002. Some new Q-value correlations to assist in site characterization and tunnel design. International Journal of Rock Mechanics and Mining Sciences, Vol. 39, No. 2, pp. 185–216, https://doi.org/10.1016/S1365-1609(02)00011-4

Basnet, C.B., Panthi, K.K., 2020. Detailed engineering geological assessment of a shotcrete lined pressure tunnel in the Himalayan rock mass conditions: a case study from Nepal. Bulletin of Engineering Geology and the Environment. No. 79, pp. 153–184, https://doi.org/10.1007/s10064-019-01544-9

Bieniawaski, Z.T., 1978. Determining rock mass deformability: Experience from case histories. International Journal of Rock Mechanics and Mining Sciences & Geomechanics Abstracts, Vol. 15, No. 5, pp. 237–247, https://doi.org/10.1016/0148-9062(78)90956-7

Bieniawaski, Z.T., 1993. Classification of rock masses for engineering: The RMR-system and future trends. Comprehensive rock engineering, J. A. Hudson ed., Vol. 3, pp. 553–573, https://doi.org/10.1016/B978-0-08-042066-0.50028-8

Hoek, E., Torres, C. C. and Corkum, B., 2002. Hoek-Brown failure criterion – 2002 edition. Proceedings North American Rock Mechanics Society Meeting. Toronto, Canada.

Hoek, E., 2007. Practical Rock Engineering. www.rocscience.com

Hoek, E., Carter, T.G. and Diederichs, M.S. 2013. Quantification of the Geological Strength Index Chart. 47th US Rock Mechanics/Geomechanics Symposium, San Francisco, CA, USA

Katuwal, T.B., Panthi, K.K. & Basnet, C.B., 2023. Challenges associated with the construction of vertical and inclined shafts in the Himalayan Region. ISRM 15th International Congress on Rock Mechanics and Rock Engineering – Challenges in Rock Mechanics and Rock Engineering, Salzburg, Austria, ISBN 978-3-9503898-3-8

Khatri, D.B., Zhang, W., Fang, X., Meng, Q., Zhang, T., Zhang, D. and Paudayal, K.N., 2021. Rock Magnetism of Late Cretaceous to Middle Eocene Strata in the Lesser Himalaya, Western Nepal: Inferences Regarding the Paleoenvironment. Frontiers in Earth Sciences, Vol. 9, pp. 1–15, https://doi.org/10.3389/feart.2021.744063

Panthi, K.K., 2006. Analysis of engineering geological uncertainties related to tunnelling in Himalayan rock mass conditions. Doctoral Thesis, Norwegian University of Science and Technology 2006: 41, Norway, ISBN 82-471-7825-7

Panthi, K.K. and Nilsen, B., 2007. Uncertainty analysis of tunnel squeezing for two tunnel cases from Nepal Himalaya. International Journal of Rock Mechanics & Mining Sciences, Vol. 44, No. 1, pp. 67–76, https://doi.org/10.1016/j.ijrmms.2006.04.013

Panthi, K.K. and Basnet, C.B., 2018. A dynamic analysis of in-situ stress state at the Upper Tamakoshi Hydroelectric Project area, Nepal. Hydro Nepal: Journal of Water, Energy and Environment, No. 23, pp. 42–47, https://doi.org/10.3126/hn.v23i0.20824

Panthi, K.K., 2012. Evaluation of rock bursting phenomena in a tunnel in the Himalayas. Bulletin of Engineering Geology and the Environment, No. 71, pp. 761–769, https://doi.org/10.1007/s10064-012-0444-5

Panthi, K.K., 2017. Rockburst prediction methods and their applicability. Rock Burst - Mechanism, Monitoring, Warning and Mitigation Elsevier/Butterworth-Heinemann, pp. 381–385

Panthi, K.K., 2018. Super Dordi KHA Hydropower Project in Nepal Follow up and Field Visit Report, Department of Geosciences and Petroleum, NTNU Norway.

PHCPL, 2012. Project Summary & Memorandum of Information. Synopsis Report of Dordi, Nepal, Peoples Hydropower Company (P) Ltd. pp. 1–56

Rathore, A., & Panthi, K. K., 2017. Evaluation of Powerhouse Cavern for the SachKhas Hydroelectric Project in Himachal, India. Hydro Nepal: Journal of Water, Energy and Environment, No.20, pp.23–30. https://doi.org/10.3126/hn.v20i0.16485

Robyr M., Vannay J. C., Epard J. L. and Steck A., 2002. Thrusting, extension, and doming during the polyphase tectonometamorphic evolution of the high Himalayan crystalline zone in NW India. Journal of Asian Earth Sciences, Vol. 22, No. 30, pp. 221–239, https://doi.org/10.1016/S1367-9120(02)00039-1